Degradation of integral membrane proteins modified with the photosensitive degron module requires the cytosolic endoplasmic reticulum–associated degradation pathway

Johannes Scheffer[a,†], Sophia Hasenjäger[b,†], and Christof Taxis[b,*]
[a]Department of Chemistry/Biochemistry and [b]Department of Biology/Genetics, Philipps-University Marburg, 35043 Marburg, Germany

ABSTRACT **Protein quality mechanisms are fundamental for proteostasis of eukaryotic cells. Endoplasmic reticulum–associated degradation (ERAD) is a well-studied pathway that ensures quality control of secretory and endoplasmic reticulum (ER)–resident proteins. Different branches of ERAD are involved in degradation of malfolded secretory proteins, depending on the localization of the misfolded part, the ER lumen (ERAD-L), the ER membrane (ERAD-M), and the cytosol (ERAD-C). Here we report that modification of several ER transmembrane proteins with the photosensitive degron (psd) module resulted in light-dependent degradation of the membrane proteins via the ERAD-C pathway. We found dependency on the ubiquitylation machinery including the ubiquitin-activating enzyme Uba1, the ubiquitin-conjugating enzymes Ubc6 and Ubc7, and the ubiquitin–protein ligase Doa10. Moreover, we found involvement of the Cdc48 AAA-ATPase complex members Ufd1 and Npl4, as well as the proteasome, in degradation of Sec62-myc-psd. Thus, our work shows that ERAD-C substrates can be systematically generated via synthetic degron constructs, which facilitates future investigations of the ERAD-C pathway.**

Monitoring Editor
Mark J. Solomon
Yale University

Received: Dec 3, 2018
Revised: Aug 1, 2019
Accepted: Aug 9, 2019

INTRODUCTION

The ubiquitin–proteasome system (UPS) in eukaryotic cells is fundamental for regulated proteolysis of unnecessary or damaged proteins. In humans, dysregulation of UPS activity or increased abundance of damaged proteins is connected to aging and disease development (Cuanalo-Contreras *et al.*, 2013; Vilchez *et al.*, 2014). This emphasizes the importance of the protein quality control machinery that selects damaged or misfolded proteins for degradation. Here, the first crucial step is recognition of a degradation signal (degron) that is exposed by a protein, which can be executed by ubiquitin–protein ligases (E3) or by chaperones (Ravid and Hochstrasser, 2008). Subsequently, the substrate is ubiquitylated by the E3 together with a ubiquitin-conjugating enzyme (E2); this step requires activated ubiquitin, which is provided by a ubiquitin-activating enzyme (E1; Ciechanover, 2005). Substrate polyubiquitylation then triggers targeting to the proteasome, followed by substrate unfolding and degradation. However, the proteasome itself recognizes some specific degrons, which leads to ubiquitin-independent degradation of the attached proteins (Erales and Coffino, 2014).

The photosensitive degron (psd) module contains the photoreceptor domain LOV2 from *Arabidopsis thaliana* and the synthetic ubiquitin-independent degron cODC1, which was derived from the carboxy-terminal degron of murine ornithine decarboxylase (ODC). It consists of a peptide of 37 amino acids without secondary structure comprising a cysteine–alanine motif, which is important for proteasomal degradation (Erales and Coffino, 2014). The LOV2 domain exposes cODC1 upon illumination with blue light, which triggers degradation of the whole protein by the proteasome

This article was published online ahead of print in MBoC in Press (http://www.molbiolcell.org/cgi/doi/10.1091/mbc.E18-12-0754) on August 14, 2019.
The authors declare no conflicts of interest.
†These authors contributed equally to this work.
Author contributions: J.S., S.H., and C.T. performed experiments; C.T. analyzed the data and wrote the manuscript; all authors read and approved the manuscript.
*Address correspondence to: Christof Taxis (taxis@staff.uni-marburg.de).
Abbreviations used: AAA-ATPase, ATPase associated with diverse cellular activities; cODC1, synthetic degron 1 derived from carboxy-terminus of ornithine decarboxylase; CPY, carboxypeptidaseY; ERAD, endoplasmic reticulum-associated degradation; ERAD-C, ERAD substrate with a misfolded domain in the cytosol; LOV2, light oxygen voltage domain 2 from phototropin1; psd, photosensitive degron.

(Renicke *et al.*, 2013; Trauth *et al.*, 2019). The degron cODC1 was successfully utilized to target two membrane proteins for degradation, the ER membrane protein Sec62 from *Saccharomyces cerevisiae* and the membrane protein synaptotagmin (SNT1) from *Caenorhabditis elegans* (Renicke *et al.*, 2013; Hermann *et al.*, 2015).

These findings raised the question of how these secretory proteins were targeted for destruction. The endoplasmic reticulum (ER) harbors an extensively studied machinery for protein quality control, the ER-associated protein degradation (ERAD) system. ERAD recognizes misfolded proteins in the lumen of the ER (ERAD-L), in the ER membrane (ERAD-M), and in cytosolic domains of ER membrane proteins (ERAD-C). The main components of ERAD multiprotein complexes consist of an E3, several E2s, and associated proteins.

In yeast, it has been demonstrated that the E3 ligase Hrd1 complex acts mostly in ERAD-L and ERAD-M, whereas the E3 Doa10/Ssm4 complex acts on ERAD-C substrates. There is evidence that these complexes are directly involved in export of luminal and transmembrane substrates; however, the translocon has also been implicated in this process (Zattas and Hochstrasser, 2015; Preston and Brodsky, 2017; Römisch, 2017). The cytosolic AAA-ATPase complex Cdc48-Npl4-Ufd1, which is attached to the ER membrane by the receptor protein Ubx2, is involved in transfer of ERAD substrates to the proteasome for degradation. For some substrates, it has been shown that this transfer activity is dependent on the AAA-ATPases of the proteasome itself (Mayer *et al.*, 1998; Walter *et al.*, 2001; Ye *et al.*, 2017).

Here we investigated the degradation of several ER membrane proteins modified with the photosensitive degron module and compared it with the degradation of soluble psd-modified proteins (Figure 1). This revealed that the ERAD-C pathway and the E3 Doa10 are involved in degradation of these substrates. Degradation requires an active E3 and the carboxy terminus of Doa10, which has been linked to substrate recognition (Zattas *et al.*, 2016). Furthermore, the Cdc48 complex and the AAA-ATPases of the proteasome are required for efficient degradation. Overall, our investigation has implications for degron recognition by Doa10 and by the proteasome.

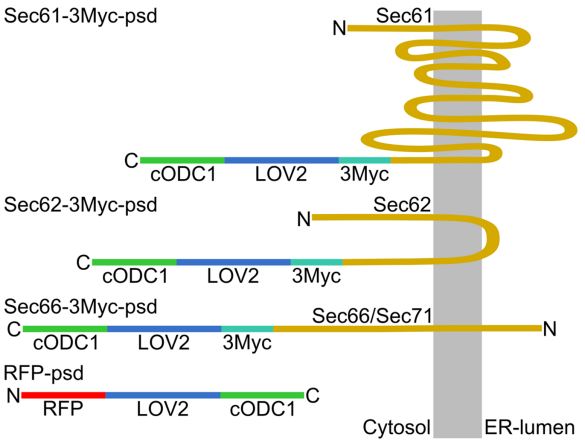

FIGURE 1: Scheme of the substrates used in this study. The essential protein Sec61 was modified at the C-terminus with a 3 Myc tag and a photosensitive degron (psd) module. The latter consists of the photoreceptor LOV2 from *Arabidopsis thaliana* phototropin 1 and a synthetic degron derived from the C-terminus of murine ornithine decarboxylase (cODC1). The degron is caged and inactive in darkness, whereas illumination of LOV2 with blue light results in exposure and activation of the cODC1 degron, which induces degradation by the proteasome. Sec61 is an integral ER-membrane protein with 10 transmembrane domains; the N- and C-terminus are localized in the cytosol. The translocon-associated protein Sec62 has two transmembrane domains and both termini in the cytosol; Sec66 has its N-terminus in the ER and the C-terminus in the cytosol. The substrates were modified at the C-terminus with the psd module. As cytosolic control substrate, the psd module was fused to the C-terminus of the red fluorescent protein mCherry.

RESULTS

Destabilization of diverse membrane proteins by the photosensitive degron module

The psd module was developed to regulate protein stability using a conditional degron that is recognized directly by the proteasome. Previously, we observed that the ER transmembrane protein Sec62 can be targeted for degradation in a blue light–dependent manner using the psd module (Renicke *et al.*, 2013). In this study, we investigated whether modification with the psd module is a general way to control the stability of ER membrane proteins with their C-terminus exposed to the cytosol. Thus, we tagged ER membrane proteins with one, two, or 10 membrane-spanning domains with the psd module (Figure 1). The psd module was integrated at the 3′ end of the genes, resulting in strains that contained only the fusion proteins and no unmodified variant. We measured the half-life of Sec61, Sec62, and Sec66 (also referred to as Sec71) modified with the 3myc-psd module in darkness and in cells exposed to blue light by using the translational inhibitor cycloheximide (chx) to block protein synthesis. In cells kept in darkness, we measured half-lives of 20 ± 3, 18 ± 2, and 18 ± 2 min for Sec61-3myc-psd, Sec62-3myc-psd, and Sec66-3myc-psd, respectively. Exposure of the cells to blue light induced rapid protein degradation, resulting in half-lives of 4 ± 0.6 min (Sec61-3myc-psd), 1 ± 0.1 min (Sec62-3myc-psd), and 2 ± 0.3 min (Sec66-3myc-psd; Figure 2, A–C). The light-induced degradation of the membrane proteins modified with the psd module resulted in much quicker degradation than with a soluble protein tagged with the psd module. For the latter, a half-life of 20 min has been measured (Renicke *et al.*, 2013). This suggested a changed degradation mechanism, which we were interested in investigating further.

A blue light–induced growth phenotype was reported for Sec62-3myc-psd (Renicke *et al.*, 2013). Similarly, we observed that Sec61-3myc-psd cells were unable to proliferate when exposed to blue light (Supplemental Figure S1D). This suggests that the rapid degradation of Sec61-3myc-psd in cells exposed to blue light (Figure 2A) leads to greatly diminished ER-import and subsequently to loss of viability. We also checked the functionality of Sec61-3myc-psd and Sec62-3myc-psd in darkness and in cells exposed to blue light by visualizing carboxypeptidaseY (CPY) and its precursors by immunoblotting. CPY is synthesized as preproCPY (cytosolic, 60 kDa) and posttranslationally imported into the ER. There, the signal sequence is cleaved off and the protein is glycosylated, resulting in proCPY, with a molecular mass of 67 kDa (p1CPY). The carbohydrates are processed in the Golgi, resulting in the p2CPY form (69 kDa). In the vacuole, CPY is processed to the active protease (mCPY, 61 kDa) by proteolysis (Rendueles and Wolf, 1988). This showed that a certain amount of cytosolic preproCPY is already present in darkness in both cases, suggesting diminished activity of Sec61 and Sec62 after modification with the psd module (Supplemental Figure S1E). Interestingly, we did not observe a pronounced increase of preproCPY in cells exposed to blue light. This may be explained by the constitutive degradation of preproCPY in the cytosol (Metzger *et al.*, 2008). Then, we checked whether the modification of Sec61, Sec62, and Sec66 with the 3myc-psd module disturbed membrane integration

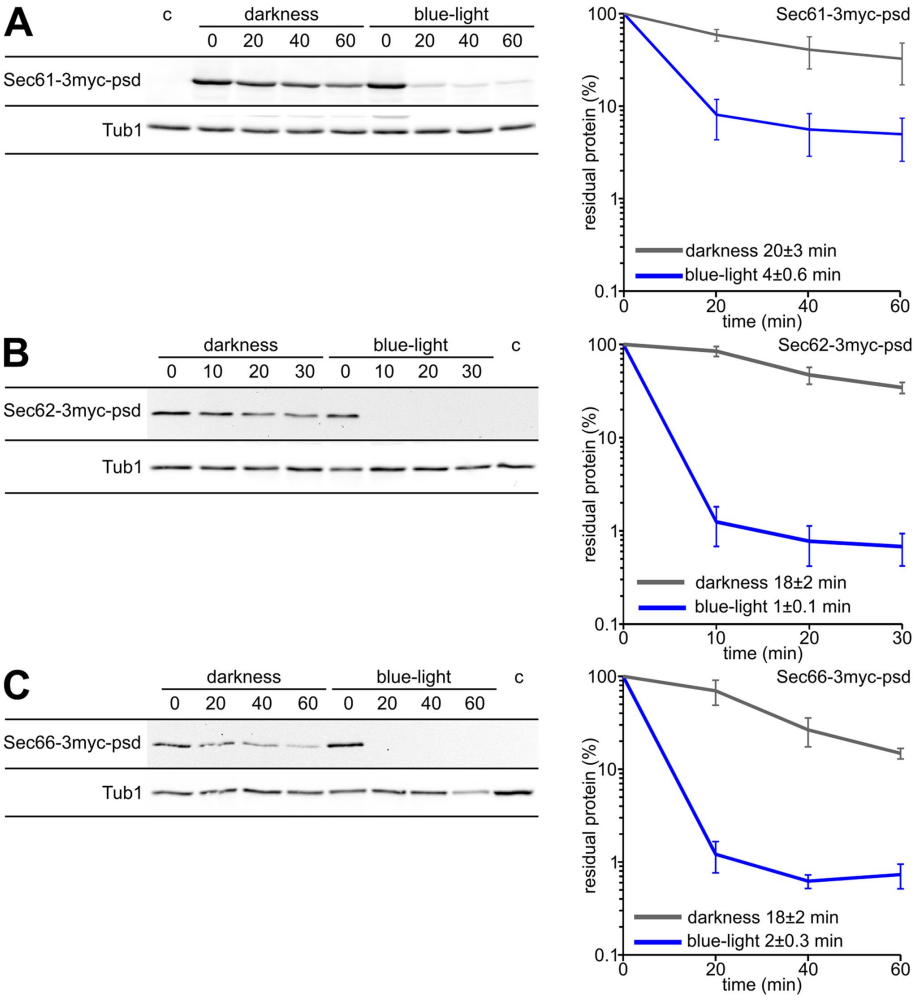

FIGURE 2: Degradation kinetics of ER membrane proteins modified with the psd module. (A) Cycloheximide chase analysis of Sec61 modified with a psd tag (YDS462). A strain without psd module was used to assess antibody specificity (c = negative control, yeast strain SUB62). The translational inhibitor cycloheximide (chx) was used to stop protein synthesis after removal of the first sample (t = 0 min). Cells were exposed to blue light (465 nm, 30 µmol m^{-2} s^{-1}) after addition of chx. Samples taken at the indicated time points were subjected to alkaline lysis and immunoblottting. Antibodies directed against Myc and Tub1 (loading control) were used for detection. The immunoblot shows an illustrative result. The graph at the bottom shows quantification of four independent experiments (n = 4; error bars indicate SEM). The complete membrane with molecular size markers is shown in Supplemental Figure S1A. (B, C) Cycloheximide chase analysis of Sec62 (YDS174) and Sec66 (YDS189) modified with a psd tag. Experimental conditions as in A. The complete membranes with molecular size markers are shown in Supplemental Figure S1, B and C.

using a carbonate extraction assay. This showed profound solubilization of the psd-modified proteins only with 1% Triton X-100, which suggests that the proteins are embedded in a membrane (Supplemental Figure S1F). As the strains that carry only Sec61-3myc-psd or Sec62-3myc-psd are viable in darkness, it can be concluded that these proteins are functional transmembrane proteins.

Degradation of Sec62-3myc-psd requires proteasomal AAA-ATPases

We selected Sec62-3myc-psd as a model substrate to investigate the light-induced degradation of ER membrane proteins modified with the psd module in more detail. First, we tested degradation of Sec62-3myc-psd in yeast strains with mutations in the invariant lysine of the Walker A motif of the proteasomal AAA-ATPases *RPT1-6* (Rubin *et al.*, 1998). Degradation assays using murine ODC as substrate have shown that an *rpt4* mutant had the most profound impact, although the assays did not result in a complete degradation block (Erales *et al.*, 2012). In agreement with these observations, we found a slight delay in Sec62-3myc-psd degradation in the *rpt6* mutant and a stronger impact in the *rpt4* mutant (Figure 3, A and B). In the viability assay, only the *rpt4* strain was able to grow under blue-light illumination (Figure 3C). This demonstrates that proteasomal activity is important for Sec62-3myc-psd degradation.

The Cdc48-Npl4-Ufd1 complex is required for degradation of Sec62-3myc-psd

Second, we tested whether other cytosolic factors besides the proteasome are involved in degradation of Sec62-3myc-psd. The AAA-ATPase Cdc48 and its complex partners Npl4 and Ufd1, as well as their membrane anchor Ubx2, have a general impact on degradation of ubiquitylated ERAD substrates by the proteasome. We used the *ufd1-1*, *npl4-1*, and *ubx2*Δ mutants to assess involvement of this complex in Sec62-3myc-psd degradation. The assays revealed that Ufd1 and Npl4 are necessary for efficient degradation of Sec62-3myc-psd (Figure 4A). The impact of the mutations on Sec62-3myc-psd proteolysis was profound enough to allow growth of the *ufd1* and *npl4* mutant strains exposed to blue light (Figure 4B). Similarly, deletion of *UBX2* prolonged the half-life of Sec62-3myc-psd in blue light and allowed growth of the strain exposed to blue light, although at a lower rate than in the isogenic control strain (Figure 4, C and D). Presumably, Sec62-3myc-psd stabilization in the absence of Ubx2 under blue-light conditions is not profound enough to reach normal Sec62 levels. This may result in secretory pathway problems that manifest in a slow-growth phenotype under restrictive conditions. The involvement of the Cdc48-Ufd1-Npl4 complex and its membrane receptor Ubx2 in degradation of Sec62-3myc-psd indicated that a ubiquitylation step might be part of the degradation process.

Sec62-3myc-psd degradation depends on the E3 Doa10

Next, we tested ERAD E3s Doa10 and Hrd1, as well as ERAD component Hrd3. The assays revealed strong stabilization of Sec62-3myc-psd in *doa10*Δ cells, whereas absence of Hrd1 or Hrd3 had no impact (Figure 5A). Quantification showed no degradation of Sec62-3myc-psd in the *doa10*Δ mutant strain (Figure 5B). Moreover, the *doa10*Δ strain was growing robustly when exposed to blue light (Figure 5C). In addition, we tested the involvement of other known ERAD components, such as the yeast derlins, as well as the translocon, in degradation of Sec62-3myc-psd using a *der1*Δ *dfm1*Δ

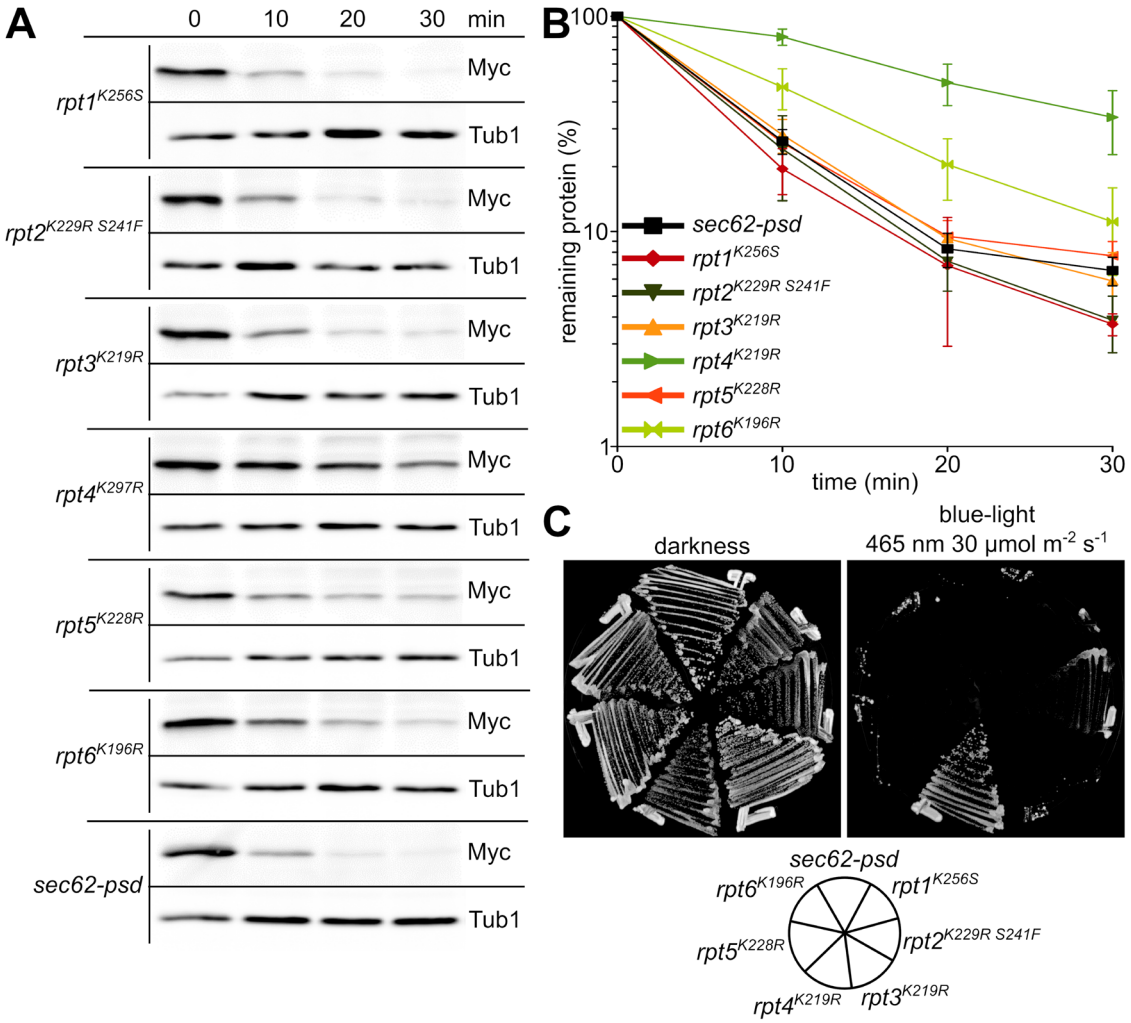

FIGURE 3: Light-induced depletion of Sec62-3myc-psd requires functional AAA-ATPases of the proteasome. (A) Cycloheximide chase analysis of strains with defective proteasomal AAA-ATPases. Experimental conditions as in Figure 2A using strains YDS232 (*sec62-3myc-psd*), YDS224 (*rpt1*), YDS235 (*rpt2*), YDS223 (*rpt3*), YDS230 (*rpt4*), YDS228 (*rpt5*), and YDS227 (*rpt6*), all containing *sec62-3myc-psd*. (B) Quantification of the immunoblots shown in A. The graph shows the mean of three independent experiments (error bars, SEM). (C) Streaks of the yeast strains used in A on YPD plates. The plates were incubated at 30°C for 2 d and exposed to blue light (as indicated) or kept in darkness.

double mutant, a *sec61-2* mutant, and a *sbh1*Δ *sbh2*Δ double mutant. However, neither the derlins (Supplemental Figure S2) nor the translocon mutants (Supplemental Figure S3) had an impact on Sec62-3myc-psd degradation.

Next, we investigated whether Doa10 was involved in degradation of Sec62-3myc-psd in its capacity as an E3 using a mutant with a cysteine-to-serine exchange in the RING finger domain (Doa10^{C39S}). Similarly to the results with a full-deletion mutant, we found a block in Sec62-3myc-psd degradation (Figure 6A). The viability assay confirmed this result: the RING finger mutation allowed growth of a Sec62-3myc-psd-containing strain exposed to blue light (Figure 6B). Recently, the cytosolic C-terminus of Doa10 has been implicated in recognition of transmembrane and soluble substrate proteins (Zattas *et al.*, 2016). We replaced this C-terminal tail of Doa10 with 3mCherry and investigated the degradation of Sec62-3myc-psd. Again, we found complete stabilization of light-induced degradation of Sec62-3myc-psd and growth of the mutant strain under Sec62-3myc-psd–destabilizing conditions (Figure 6, C and D). The immunodetection of Doa10 and ofDoa10C with antibodies against mCherry show similar protein amounts for both Doa10 variants (Figure 6C); however, the interpretation is hindered by the appearance of multiple bands. These might indicate partial Doa10 degradation or might originate from mCherry disintegration during SDS–PAGE sample preparation, which has been documented (Gross *et al.*, 2000). Furthermore, we tested Doa10 involvement in the degradation of Sec61-3myc-psd and Sec66-3myc-psd. Both proteins are located in the ER membrane with multiple transmembrane domains (Sec61) or a single transmembrane-spanning region (Sec66; Figure 1). Similarly, we found nearly complete stabilization of these substrates in the absence of Doa10, demonstrating that the number of transmembrane segments does not influence the degradation process (Supplemental Figure S4, A and B). In conclusion, Doa10 activity and its potential substrate recognition domain are necessary for degradation of psd-modified ER-membrane proteins.

Sec62-3myc-psd degradation is dependent on ubiquitylation machinery

The ODC-like degron and a critical cysteine residue, which is located in the central part of the degron sequence, are essential components for efficient proteasomal degradation of cytosolic proteins

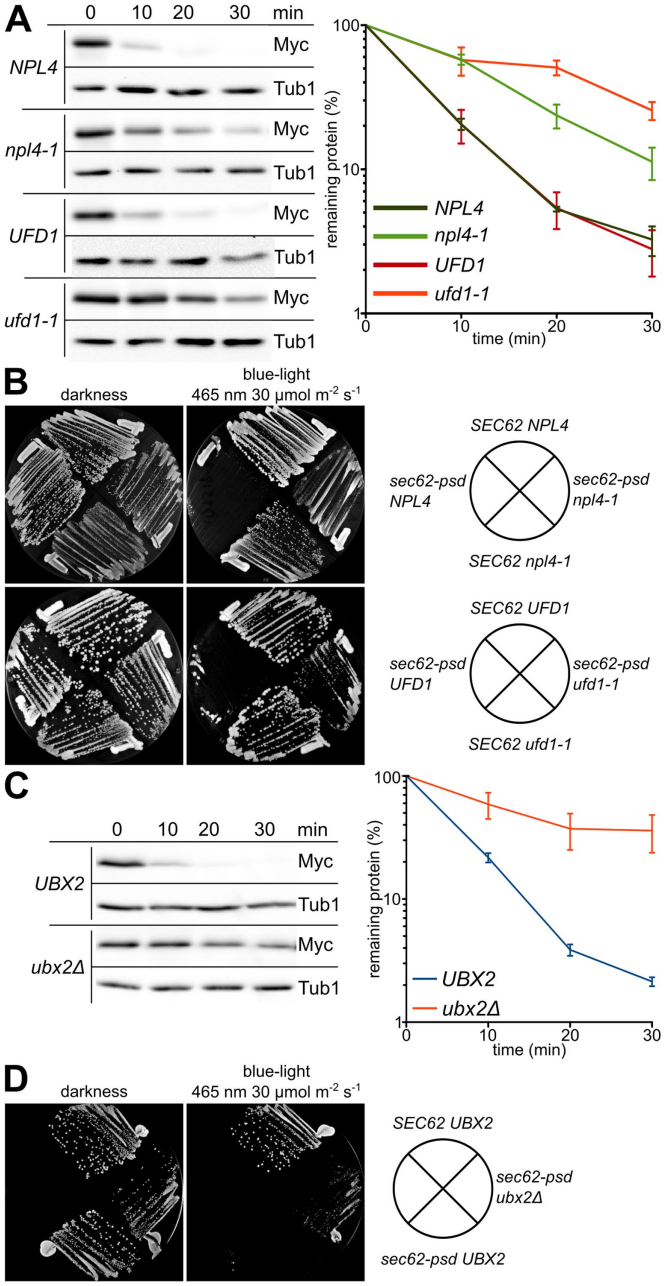

FIGURE 4: The Cdc48-Npl4-Ufd1 complex and its ER membrane anchor Ubx2 are involved in Sec62-3myc-psd degradation. (A) Cycloheximide chase analysis of a *NPL4* control strain (YDS278), an *npl4-1* mutant strain (YDS288), a *UFD1* control strain (YDS289), and a *ufd1-1* mutant strain (YDS285), all containing Sec62-3myc-psd. Experimental conditions as in Figure 2A, but performed at room temperature. The graph shows the mean of four independent experiments (error bars, SEM). (B) Streaks of the yeast strains shown in A and a wild-type *NPL4* strain (FY23), an *npl4-1* mutant strain (PSY2340), a wild-type *UFD1* strain (YCT397), and a *ufd1-1* mutant strain (YCT415) without Sec62-3myc-psd. Experimental conditions as in Figure 3C, but the strains were incubated at room temperature. (C) Cycloheximide chase analysis of a *UBX2* control strain (YDS174) and a *ubx2*Δ deletion strain (YDS305), both containing Sec62-3myc-psd. Experimental conditions as in Figure 2A. The graph shows the mean of four independent experiments (error bars, SEM). (D) Streaks of the yeast strains shown in C and a wild-type strain (YDS28) without Sec62-3myc-psd. Experimental conditions as in Figure 3C.

modified with the psd module (Renicke *et al.*, 2013; Usherenko *et al.*, 2014). We fused a variant of the psd module to Sec62 that carries a cysteine-to-alanine exchange at this position. Compared with the original psd construct, Sec62-3myc-psd^{CA} degradation was slowed down and the mutant strain was able to grow slowly when exposed to blue light (Figure 7, A and B).

Next, we tested the dependency of Sec62-3myc-psd degradation on ubiquitylation machinery using an *uba1^{ts}* mutant strain (Palanimurugan *et al.*, 2004). This revealed that Sec62-3myc-psd degradation was delayed in an *uba1^{ts}* mutant under restrictive conditions and that this strain was able to grow while exposed to blue light (Figure 8, A and B).

Moreover, we tested the impact of the ubiquitin-conjugating enzymes Ubc6 and Ubc7 on Sec62-3myc-psd degradation. These E2s are the regular partners of Doa10 during degradation of ERAD substrates (Swanson *et al.*, 2001). The assay revealed that Sec62-3myc-psd degradation was completely blocked in the absence of Ubc6 or Ubc7 and in a double mutant lacking both E2s (Figure 8C). In addition, absence of the E2s allowed the growth of the Sec62-3myc-psd strain (Figure 8D). These results demonstrate that degradation of Sec62-3myc-psd required ubiquitylation by Doa10. Next, we investigated whether ubiquitylated Sec62-3myc-psd is detectable after a short pulse of blue light. We found strong accumulation of polyubiquitylated Sec62-3myc-psd in *rpt4^{K297R}* mutants, whereas in Sec62-3myc-psd control cells and in a strain lacking *DOA10*, only few ubiquitylated proteins were precipitated with Myc-specific antibodies (Figure 9). Quantification revealed that in *doa10*Δ cells the amount of precipitated material detected by the α-ubiquitin antibody was even smaller than that in the control cells, which underlines the role of Doa10 as critical E3 for Sec62-3myc-psd degradation.

In comparison to Sec62-psd, we investigated the degradation behavior of soluble fluorescent proteins fused to the psd to assess whether these proteins rely on a similar degradation pathway as membrane proteins fused to psd. We followed the degradation of GFP-3myc-psd in cells impaired in proteasomal degradation (*pre1-1 pre2-2* and *pre1-1 pre4-1*) and corresponding control cells. As expected, we found strong impairment of blue-light induced degradation in the proteasome mutants for GFP-3myc-psd (Figure 10A). In comparison with the transmembrane proteins modified with 3myc-psd, the soluble psd substrate is degraded with slower degradation kinetics upon blue-light exposure in otherwise wild-type cells.

Then we investigated the degradation of RFP-psd and RFP-psd^{CA} in cells lacking the E3 *DOA10*, as well as in the corresponding control cells. This revealed a slower degradation of RFP-psd^{CA} than of RFP-psd in control cells (Figure 10B). Unexpectedly, we also observed a profound influence of Doa10 on the degradation of RFP-psd and RFP-psd^{CA}. Interestingly, the cysteine–alanine mutation had a stronger impact than the absence of Doa10 on RFP-psd degradation, which suggests that the degradation depends mostly on ubiquitin-independent degradation induced by the cODC1 degron. Nevertheless, RFP-psd^{CA} in *doa10*Δ cells was almost completely stable over the course of 90 min, which indicates that ubiquitylation machinery including the E3 Doa10 has a nonnegligible influence on soluble psd substrates.

To clarify the influence of the ubiquitylation machinery on degradation of soluble psd substrates, we investigated the degradation of RFP-psd in *uba1^{ts}* cells with the same strain background that has been used for the Sec62-3myc-psd degradation assay (Palanimurugan *et al.*, 2004). Also, for RFP-psd, we observed a slower degradation in *uba1^{ts}* cells than in the control cells (Figure 10C). Next, we followed RFP-psd degradation by fluorescence

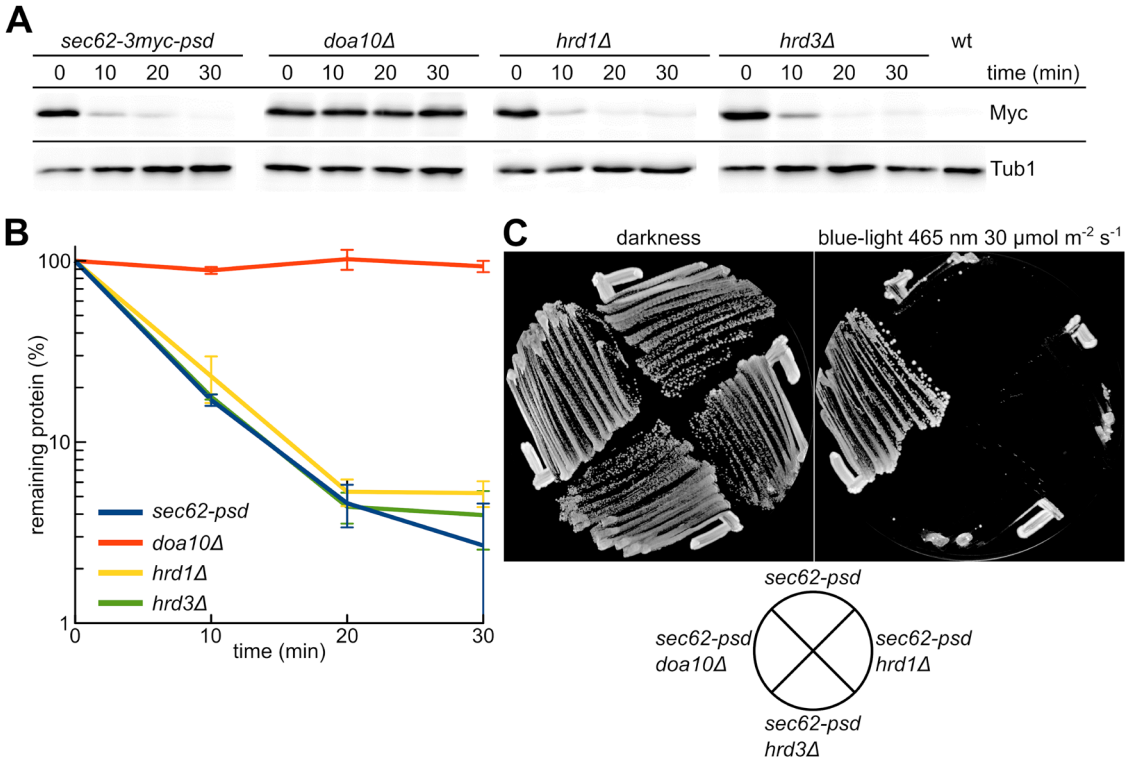

FIGURE 5: The ubiquitin–protein ligase Doa10 is necessary for depletion of Sec62-3myc-psd. (A) Cycloheximide chase analysis of strains with gene deletions of components involved in endoplasmic reticulum–associated degradation. Experimental conditions as in Figure 2A using strains YDS174 (*sec62-3myc-psd*), YDS249 (*doa10*Δ), YDS256 (*hrd1*Δ), and YDS250 (*hrd3*Δ; wt = wild-type strain BY4741). (B) Quantification of the immunoblots shown in A. The graph shows the mean of four independent experiments (error bars, SEM). (C) Streaks of the yeast strains shown in A. Experimental conditions as in Figure 3C.

measurements (Hasenjäger *et al.*, 2019). We performed a cycloheximide chase assay in control cells, as well as in *ubc6*Δ, *ubc7*Δ, *ubc6*Δ *ubc7*Δ, and *doa10*Δ mutant cells. Again, we observed the reduction in RFP-psd degradation in the *doa10*Δ cells from that in the controls, as well as reduced degradation in the strains lacking the E2s Ubc6 and Ubc7 and the double- deletion strain, which indicates that the ERAD-C pathway is involved in degradation of soluble psd substrates as well (Figure 10D).

DISCUSSION

Here, we characterized the degradation of ER transmembrane proteins modified with the psd module and demonstrated that they follow the ERAD-C pathway. This shows that such substrates can be systematically generated with the psd module. Compared to existing ERAD substrates, proteins modified with the psd module have the benefit of being conditional substrates that can be switched from a more stable conformation to a state of rapid degradation. Initially, a conditional mutant of *S. cerevisiae SEC62* was created in this way and the membrane protein SNT1 was successfully targeted in *C. elegans*, whereas the strategy was not successful for the plasma membrane protein Pma1 and the ER membrane protein Sec63 (Renicke *et al.*, 2013; Hermann *et al.*, 2015). Moreover, we tested *SEC61* and *SEC66* and found light-induced degradation in both cases. This suggests that the number of transmembrane-spanning segments is not relevant to the question of whether a transmembrane protein might be suitable for psd module-dependent generation of a conditional mutant. The translocon component Sec61 has 10 transmembrane domains, similarly to Pma1 (Wilkinson *et al.*, 1996; Ferreira *et al.*, 2002), which was found to resist light-induced degradation if modified with the psd module (Renicke *et al.*, 2013). Therefore, other reasons such as accessibility of the C-terminus might account for the difference in successful application of the psd module. The structures of the eukaryotic translocon complex and the yeast posttranslational Sec protein-translocation channel complex are available (Voorhees *et al.*, 2014; Braunger *et al.*, 2018; Itskanov and Park, 2018; Wu *et al.*, 2019). Unfortunately, the C-termini of the complex members are not all fully resolved and the structural data do not provide a clear explanation of why the psd module was successful with Sec61, Sec62, and Sec66 but not with Sec63.

To gain further insight into the degradation process, we focused on light-induced degradation of Sec62-3myc-psd. Briefly, all tested components of the ERAD-C degradation machinery were required for the degradation process, whereas components of other ERAD pathways did not influence degradation of Sec62-3myc-psd. This is in accordance with the cytosolic localization of the psd module, which makes the ERAD-C machinery the most likely candidate for degradation of Sec62-3myc-psd. However, the necessity for ubiquitylation during the degradation poses several questions how Sec62-3myc-psd is recognized at the ER membrane.

One question is how accessible cytosolic domains of ER membrane proteins are for the proteasome. Proteasome-dependent release of a transcription factor after partial proteolysis by the proteasome has been observed previously in yeast (Rape and Jentsch, 2004), which suggests susceptibility of ER membrane proteins to the

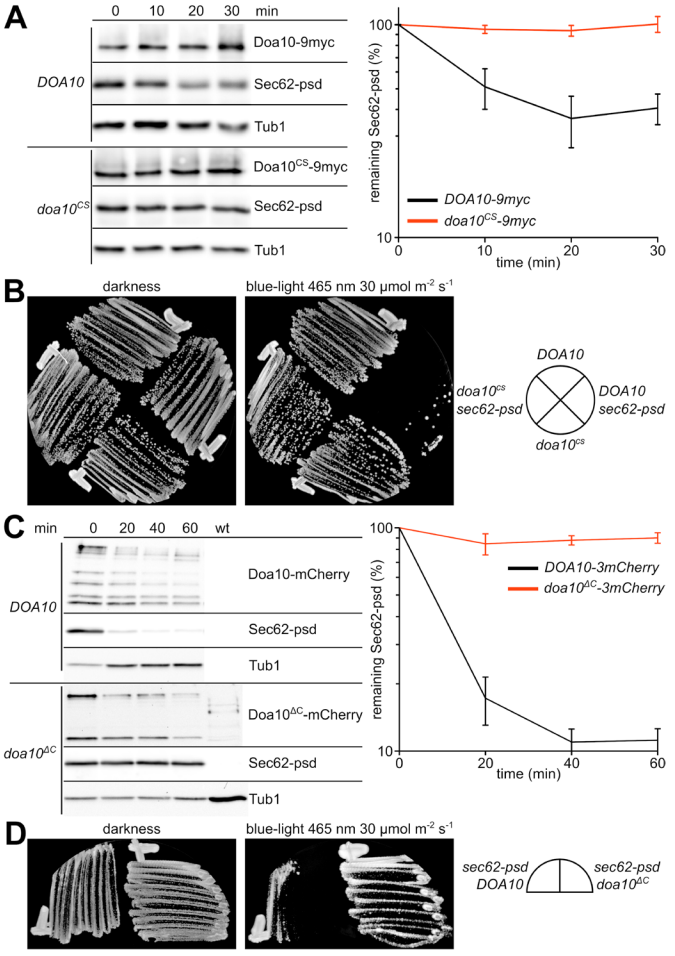

FIGURE 6: Sec62-3myc-psd degradation requires the Doa10 RING domain and the C-terminus. (A) Cycloheximide chase analysis of a *DOA10* strain (YCT1344) and a *doa10*^{CS} mutant strain (YCT1346), in which a cysteine of the RING domain has been mutated to serine. Both strains contain Sec62-3myc-psd. Experimental conditions as in Figure 2A except that Doa10-9myc and Doa10^{CS}-9myc were detected as well. The graph shows the mean of four independent experiments (error bars, SEM). (B) Streaks of the yeast strains shown in A and a *DOA10* strain (YCT1343) as well as a *doa10*^{CS} mutant strain (MHY2901), both without Sec62-3myc-psd. Experimental conditions as in Figure 3C. (C) Cycloheximide chase analysis of a control strain (YDS463) with 3mCherry-tagged Doa10 and a *doa10*$^{\Delta C}$ mutant strain (YDS453), in which the C-terminus of Doa10 has been deleted with 3mCherry (c = negative control, yeast strain MHY500). Experimental conditions as in Figure 2A except that Doa10-3mCherry and Doa10$^{\Delta C}$-3mCherry were detected as well. The multiple Doa10-3mCherry and Doa10$^{\Delta C}$ bands that are visible are most likely fragmentation products from degradation of the proteins or disintegration of mCherry during sample preparation. The graph shows the mean of four independent experiments (error bars, SEM). (D) Streaks of the yeast strains shown in C. Experimental conditions as in Figure 3C.

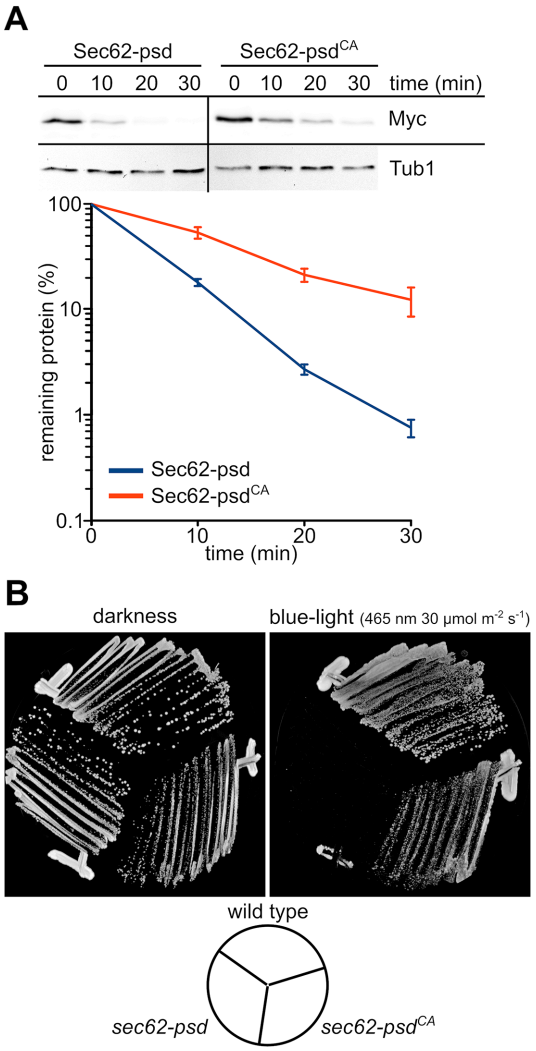

FIGURE 7: Light-induced degradation of Sec62-3myc-psd is slowed by mutating the critical cysteine of the ODC degron. (A) Cycloheximide chase analysis of Sec62 modified with a psd tag with (YDS174) or without (YDS258) active ODC degron. Experimental conditions as in Figure 2A. Illustrative result from three independent experiments is shown. The graph shows the means of Sec62-3myc-psd and Sec62-3myc-psd^{CA} stability obtained from three independent experiments. Error bars indicate SEM. (B) Streaks of the yeast strains used in A as well as a wild-type strain (ESM356-1) without modification of *SEC62* on YPD plates. Experimental conditions as in Figure 3C.

proteasome. Yet, in the absence of Doa10, in the Doa10 RING-finger mutant or in *ubc6* and *ubc7* mutants, Sec62-3myc-psd was completely stabilized. Partial proteolysis of the psd module and associated cytosolic parts of Sec62 was not observable. Thus, the psd module is inaccessible for the proteasome. Either molecular restrictions in the vicinity of the ER membrane or masking of the ODC-like degron by other proteins; for example, chaperones hinder proteolysis of the psd module at the ER membrane. Chaperones of the Hsp70 and Hsp40 families have been found to be involved in ERAD of diverse substrates; during ERAD-C, substrate ubiquitylation seems to rely on chaperone action (Zhang *et al.*, 2001; Taxis *et al.*, 2003; Han *et al.*, 2007; Nakatsukasa *et al.*, 2008; Stolz and Wolf, 2010). The lack of proteasomal proteolysis or the inaccessibility of the Sec62-3myc-psd module is remarkable, as it is clearly different from a soluble cytosolic psd-modified substrate, which is accessible to proteasomal degradation as well in the absence of ERAD-C components. The C-terminal cytosolic parts of the three substrates Sec61, Sec62, and Sec66 are of different length (~20, 70, and 150 residues, respectively). However, how accessible these C-termini are is not clear. The tagged proteins are functional, as suggested by the robust growth of Sec61-3myc-psd and Sec62-3myc-psd in darkness.

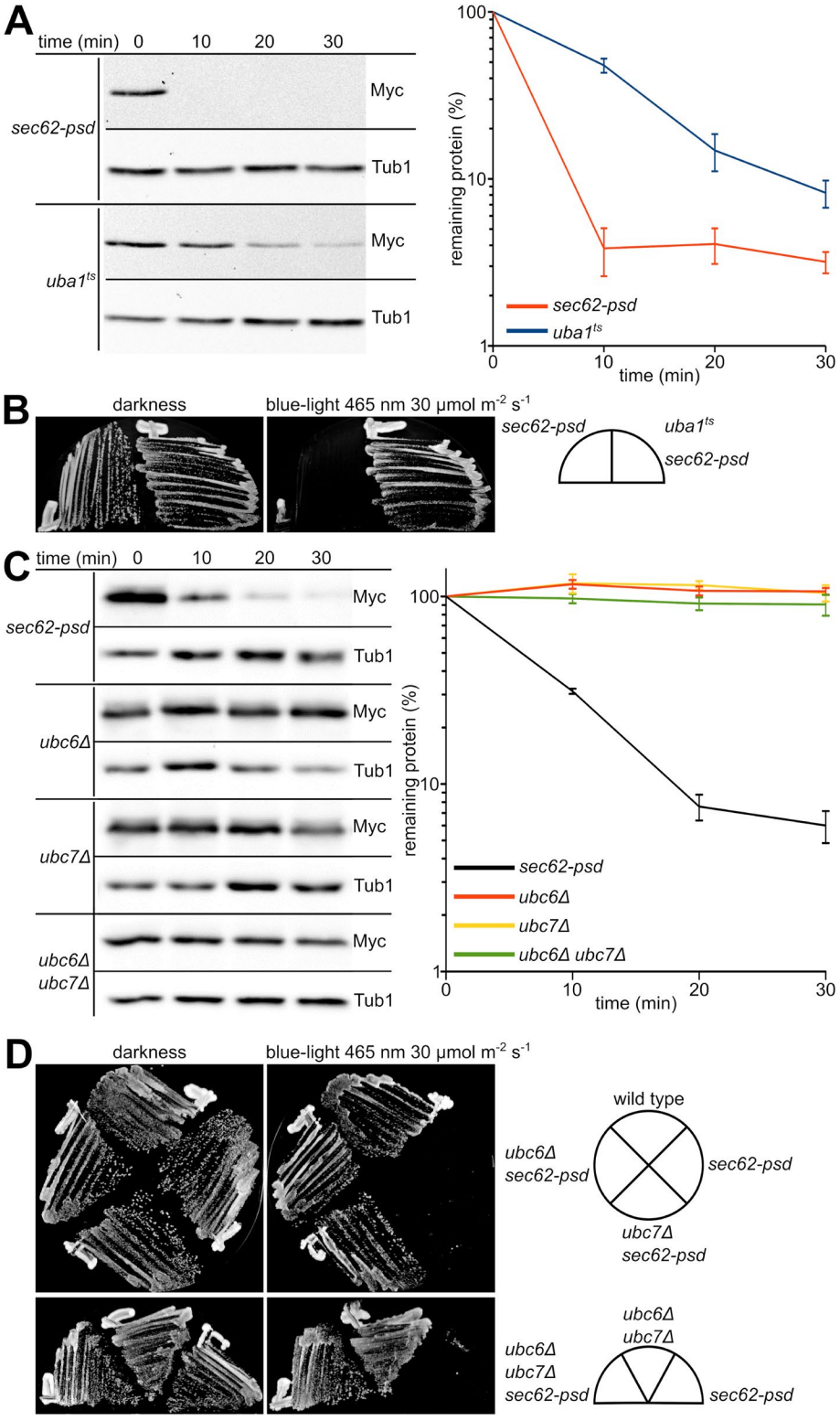

FIGURE 8: Uba1 activity and the ubiquitin-conjugating enzymes Ubc6 and Ubc7 are necessary for Sec62-3myc-psd degradation. (A) Cycloheximide chase analysis of a control strain (YDS455) and a *uba1*^{ts} strain (YDS456), both containing Sec62-3myc-psd. Experimental conditions as in Figure 2A, except that the cells were shifted from growth at room temperature to 37°C 1 h before the first sample was taken. The graph shows the quantification of four independent experiments (error bars, SEM). (B) Streaks of the yeast strains shown in A. Experimental conditions as in Figure 3C. (C) Cycloheximide chase analysis of a control strain (YCT1342), a *UBC6* deletion strain (YCT1348), a *UBC7* deletion strain (YCT1347), and a *UBC6 UBC7* double-deletion strain (YCT1350), all containing Sec62-3myc-psd. Experimental conditions as in Figure 2A. The graph shows the mean of three independent experiments (error bars, SEM). (D) Streaks of the yeast strains shown in C and an additional wild-type strain (MHY501), as well as a *UBC6 UBC7* deletion strain (MHY552), both without Sec62-3myc-psd. Experimental conditions as in Figure 3C.

Because the proteins are embedded in larger complexes to fulfill their cellular role, direct access by the proteasome could be reduced. Ubiquitylation might be a trigger for processing by the Cdc48-Npl4-Ufd1 complex, resulting in excavation of the modified subunit out of the translocon complex, as has been suggested for other Cdc48-Npl4-Ufd1-dependent substrates (Ye *et al.*, 2017). Subsequently, the Cdc48-Npl4-Ufd1 complex facilitates transfer to the cytosol, followed by proteasomal degradation.

Our data indicate that the Cdc48-Npl4-Ufd1 complex is involved in Sec62-3myc-psd degradation. However, whether it is solely responsible for the membrane-extraction step is less clear. We observed complete stabilization for mutants that interfere with ubiquitylation of Sec62-3myc-psd, whereas in the case of the Cdc48-Npl4-Ufd1 complex and the *ubx2*Δ mutant, only partial stabilization was observed. This might be because of incomplete penetration of these mutants or because of partial rescue by the AAA-ATPases of the proteasome. In the case of Ubx2, removal of the membrane anchor for the Cdc48-Npl4-Ufd1 complex might not be enough to inhibit the membrane extraction activity of the complex completely. Degradation of diverse ERAD substrates such as malfolded carboxypeptidase Y (CPY*), Hmg-CoA-reductase (HMGR), and Ole1 depends on the Cdc48-Npl4-Ufd1 complex (Bays *et al.*, 2001; Ye *et al.*, 2001; Braun and Matuschewski, 2002; Jarosch *et al.*, 2002; Rabinovich *et al.*, 2002). Yet parallel or sequential involvement of the Cdc48-Npl4-Ufd1 complex and the proteasomal AAA-ATPases in substrate dislocation has been suggested for ERAD (Lipson *et al.*, 2008; Bagola *et al.*, 2011; Morris *et al.*, 2014). Moreover, direct involvement of proteasomes was shown to be required for complete removal of the ERAD substrates Ubc6 and Deg1-Sec62 and mutated pre-pro α factor (Mayer *et al.*, 1998; Walter *et al.*, 2001; Lee *et al.*, 2004). Our data on Sec62-3myc-psd degradation disfavor direct involvement of the proteasome in the dislocation process. Although the mutation of the critical cysteine of cODC1 showed partial stabilization of Sec62-3myc-psd, it cannot be ruled out that this cysteine influences the recognition of the activated psd module by Doa10 as well. Furthermore, the complete stabilization of all three membrane proteins modified with psd in the absence of

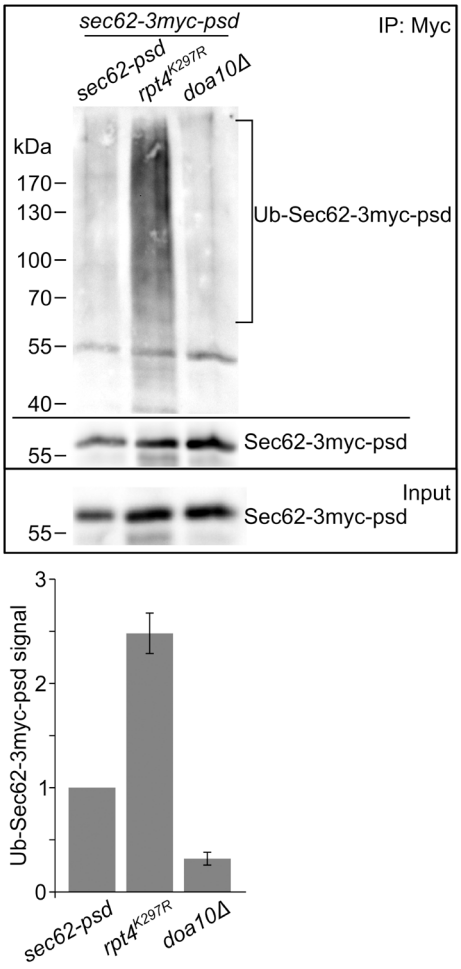

FIGURE 9: Sec62-3myc-psd is ubiquitylated by the E3 Doa10. Extracts of the strains YDS232 (control), YDS230 (*rpt4*^{K297R}), and YDS249 (*doa10*Δ) were prepared after brief blue-light illumination, subjected to Myc-directed immunoprecipitation, followed by SDS–PAGE and immunoblotting with antibodies directed against ubiquitin and the myc epitope. As a reference for substrate input, the lysates were directly analyzed as well using antibodies recognizing the Myc epitope (lower blot). The graph at the bottom shows the quantification of the signal detected with the α-ubiquitin antibody (in the blot area marked Ub-Sec62-3myc-psd) after normalization to the amount of precipitated Sec62-3myc-psd ($n = 4$; error bars, SEM).

Doa10 indicates that the proteasome is not targeting these proteins in the absence of crucial components of the ERAD-C pathway.

Interestingly, our data suggest that Sec62-3myc-psd is stabilized equally well in *UBC6* and *UBC7* deletion mutants. A similar observation has been made previously for ERAD substrate Deg1-Vma12 (Rubenstein *et al.*, 2012). Whereas both E2s team up with Doa10 for the degradation of ERAD-C substrates, Ubc7 is also part of the Hrd1 ligase complex that targets ERAD-M and ERAD-L substrates. The importance of Ubc6 and Ubc7 for substrate degradation is varying. In many substrates removal of Ubc7 has a greater impact on substrate turnover—for example, in the case of Deg1-Sec62 (Rubenstein *et al.*, 2012; Zattas and Hochstrasser, 2015). Recently, it has been shown that for Doa10 substrates the E2s have sequential activity: Ubc6 monoubiquitylates the substrate and Ubc7 extends it to a polyubiquitin chain by adding further ubiquitin molecules (Weber *et al.*, 2016). This findings explain the importance of Ubc6 for the degradation of Deg1-Vma12. In the case of Sec62-3myc-psd, a similar degradation mechanism may take place.

It is interesting to compare the proteasomal AAA-ATPase requirement for Sec62-3myc-psd degradation with other ERAD substrates or cytosolic proteins. For ERAD substrates CPY* and Hmg2, it was shown that in *rpt2RF* and *rpt4R* mutants considerable stabilization takes place (Lipson *et al.*, 2008). Furthermore, a moderate stabilization has been observed for CPY* in the *rpt6R* mutant in the same study. We found profound stabilization in the *rpt4R* mutant and slight stabilization in *rpt6R*. With a different set of *RPT*-mutants, it was observed that FLAG-tagged murine ODC degradation requires functional Rpt4 and Rpt5 (Erales *et al.*, 2012). Such subtle differences in RPT-mutants have been explained by the individual Rpt subunits facilitating the recognition and degradation of different substrate subsets (Bar-Nun and Glickman, 2012).

An interesting point is to compare the degradation mechanism of the membrane-anchored psd module with the soluble cytosolic psd module fused to a fluorescent protein. Unexpectedly, the latter showed partial dependency on ubiquitylation machinery, whereas the former seems to be completely protected from proteasomal recognition in the absence of components of the ERAD-C machinery necessary for ubiquitylation of psd-modified membrane proteins. Switches in degradation requirements have been observed before, such as for ERAD substrate Deg1-Sec62. Association of Deg1-Sec62 with the translocon induced Hrd1-dependent degradation of Deg1-Sec62, whereas mutational disruption of the affinity to the translocon resulted in Doa10 dependent degradation (Rubenstein *et al.*, 2012). Similarly, addition of a transmembrane anchor to Deg1 resulted in Cdc48-dependent degradation of Deg1-Vma12, whereas soluble Deg1 fusion proteins were degraded independent of the Cdc48-Npl4-Ufd1 complex (Ravid *et al.*, 2006).

Interestingly, the full stabilization of Sec62-3myc-psd in mutants of the ERAD-C ubiquitylation machinery (Doa10, Ubc6, and Ubc7) indicates that the psd module is not recognized or not processed by the proteasome under these conditions. This implies that the ODC-like degron is masked selectively in the membrane-anchored psd module by a factor that does not bind soluble psd modules or that access of proteasomes to membrane-bound psd is otherwise prohibited. The former model is supported by the observation that during usage of a reconstituted in vitro ERAD-C system, active Hsp70 could be provided only by the microsomal fraction and not by wild-type cytosol (Nakatsukasa *et al.*, 2008). Among others, the author proposed a model with a membrane-associated chaperone complex that sterically restricts cytosolic factors. The masking of the psd module from the proteasome might be another hint for such a model. Alternatively, it has been proposed that association of the proteasome with the ER membrane may depend on the Cdc48 complex, which in turn binds to ubiquitylated ER proteins (Nakatsukasa *et al.*, 2013). Such a scenario would argue that proteasomes do not associate with the ER without targeting by the Cdc48 complex. On the basis of current knowledge about degradation of psd-modified membrane proteins, we cannot distinguish between these models. Our finding that Sec62-3myc-psd is ubiquitylated is in agreement with the latter model as well.

The use of the psd module to create conditional mutants of transmembrane proteins and the subsequent characterization of the degradation pathway have revealed that ubiquitylation is necessary for degradation of membrane proteins and also that the degradation of soluble proteins modified with the psd module is influenced by components of the ERAD-C pathway. In summary, the blue-light switch that is provided by the psd module provides an opportunity

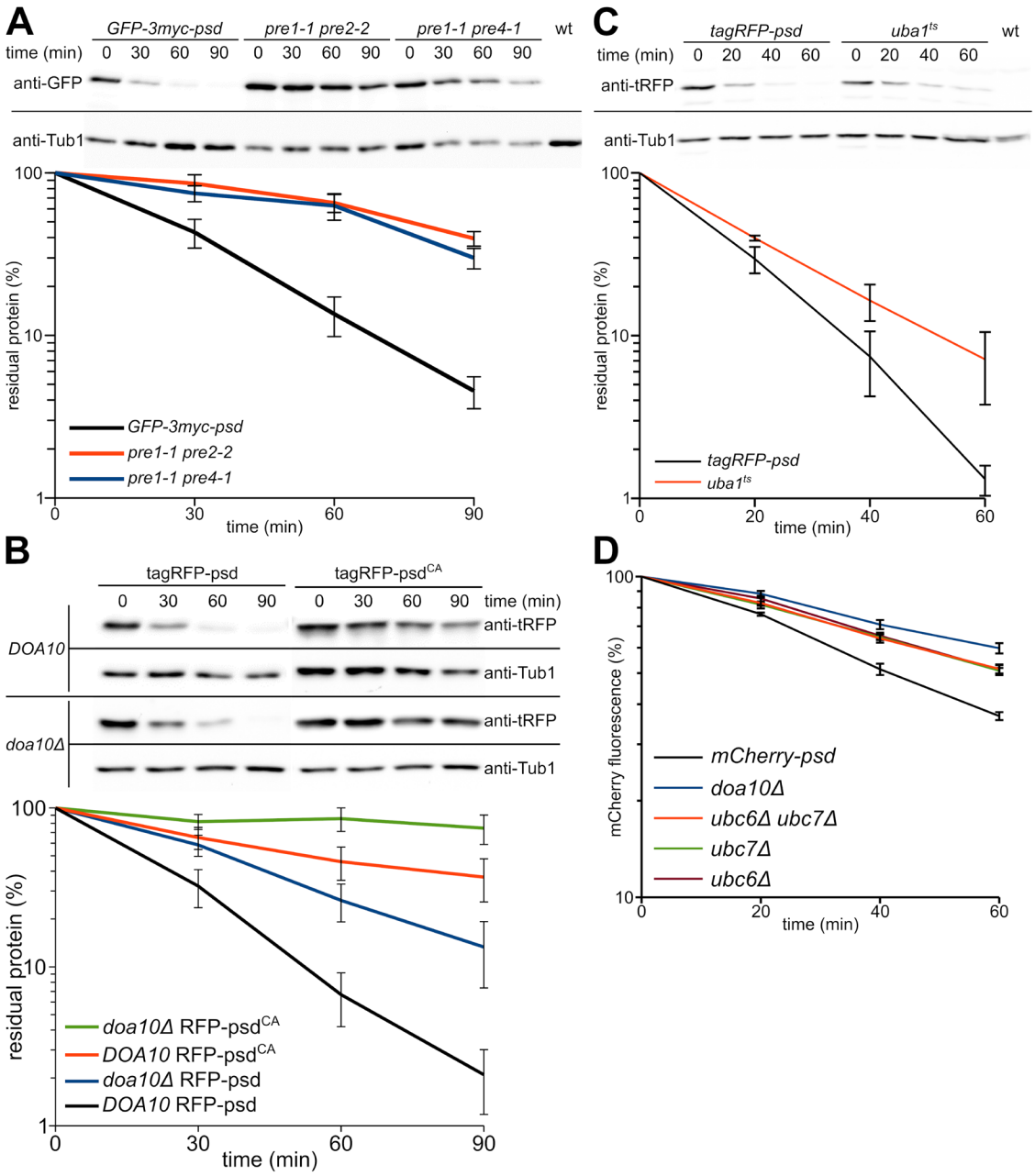

FIGURE 10: Degradation of a soluble psd substrate requires activity of ERAD-C components. (A) Involvement of the proteasome in GFP-psd degradation. Cycloheximide chase experiment (experimental conditions as in Figure 2A) using strains WCG4a, WCG4a/11/22, and YH29/14 carrying pDS112. A wild-type strain without plasmid (wt) was used as antibody control. The graph shows the mean of four independent experiments (error bars, SEM; $n = 4$). Please note the much slower degradation kinetics of the soluble GFP-3myc-psd (chase time 90 min) compared with Sec61-3myc-psd, Sec62-3myc-psd, and Sec66-3myc-psd (chase time usually 30 min). (B) Cycloheximide chase analysis to assess the involvement of the critical cysteine and the E3 Doa10 in tagRFP-psd degradation. Experimental conditions as in A using strains BY4741 (*DOA10*) and YHUM1137 (*doa10*Δ) carrying pCT334 (RFP-psd) or pDS87 (RFP-psd^{CA}). Error bars, SEM; $n = 4$. (C) Ubiquitylation is necessary for efficient tagRFP-psd degradation. Experimental conditions as in A using strains JD47 (wild type) and JD77 (*uba1*^{ts}) containing plasmid pCT334, except that the strains were grown at room temperature and then shifted to the restrictive temperature of 37°C for 1 h before the start of the chase. Error bars, SEM; $n = 3$. (D) The ubiquitin-conjugating enzymes Ubc6 and Ubc7 are involved in mCherry-psd degradation. For the cycloheximide chase experiment, cells were treated as described in Figure 2A. The samples were treated with sodium azide (10 mM end concentration) and subjected to flow cytometry. The plasmid pDS252 was used to express *mCherry-psd* in the strains MHY501 (wild type), MHY552 (*ubc6*Δ *ubc7*Δ), MHY1631 (*doa10*Δ), YCT1347 (*ubc7*Δ), and YCT1348 (*ubc6*Δ). Error bars, SEM; $n = 6$.

for novel investigations of the ERAD-C protein quality–control machinery.

MATERIALS AND METHODS

Yeast strains and growth conditions

The *S. cerevisiae* strains are derivatives of ESM356-1 and BY4741 (Brachmann *et al.*, 1998; Pereira *et al.*, 2001), as well as FY23, BWG1-7a, Sub62, MHY500, MHY501, JD47-13C, and W303 (Finke *et al.*, 1996; Rubin *et al.*, 1998; Swanson *et al.*, 2001; Jarosch *et al.*, 2002; Gödderz *et al.*, 2011). The *uba1*^{ts} strain and its control strain were shifted to the restrictive condition of 37°C 1 h before the harvesting of the first sample. Plate-growth assays were done as described (Renicke *et al.*, 2013; Usherenko *et al.*, 2014). Standard preparations of media were used for growth on plates (Sherman, 2002). Yeast cells were transformed with plasmids by the lithium acetate method (Gietz *et al.*, 1992). Low-fluorescence medium was used to grow yeast cells in liquid cultures exposed to blue light using standard plastic cell culture flasks (Usherenko *et al.*, 2014). Modification of yeast genes with the *psd* module at chromosomal level was performed as described using plasmid pDS96 as template (Lutz *et al.*, 2016). Thus, all psd-modified variants of *SEC61*, *SEC62*, and *SEC66* are the sole copies of these genes. Chromosomal taggings and gene deletions were performed as described by Janke *et al.* (2004).

Immunoblotting, antibodies, ubiquitylation assay, carbonate extraction, and statistics

Cycloheximide chases and immunoblotting were done as described previously (Renicke *et al.*, 2013; Usherenko *et al.*, 2014). Antibodies were obtained from commercial suppliers:; mouse α-Myc (clone 9E10; Cell Signalling, Danvers, MA); rabbit α-tRFP (Evrogen, Moscow, Russia); rabbit α-Tub1 (Abcam, Cambridge, UK); HRPO-conjugated secondary antibodies (Dianova, Hamburg, Germany). Detection was performed with a Chemostar professional imaging device (INTAS, Göttingen, Germany). Representative images and image quantification were obtained with the help of the software Fiji (Schindelin *et al.*, 2012) by inverting gray values and adjusting brightness and contrast as well as using the blot quantification tool.

The ubiquitylation assay was performed essentially as described by Weber *et al.* (2016). Briefly, cells in exponential growth phase (culture size 50 ml) were harvested, washed with 4 ml of cold H_2O containing 1 mM phenylmethylsulfonyl fluoride (PMSF), 10 mM NaN_3, and 20 mM N-ethyl maleimide (NEM) and lysed with glass beads in lysis buffer (6 M urea, 50 mM Tris/HCl, pH 7.5, 150 mM NaCl, 1% SDS, 1 mM PMSF, 20 mM NEM, and Roche complete inhibitor mix). Cell debris was removed by centrifugation and the lysate was diluted with nine volumes of IP dilution buffer (55 mM Tris/HCl, pH 7.5, 165 mM NaCl, 5.5 mM EDTA, 1.1% Triton X-100, 1 mM PMSF, 20 mM NEM, and Roche complete inhibitor mix). The input control was removed and 40 µl of ANTI-Myc Affinity Gel (Sigma-Aldrich) was added. The samples were placed overnight on an orbital shaker at 4°C. The samples were subjected to centrifugation and the supernatant was removed. The affinity gel was washed five times with IP dilution buffer. The affinity gel was treated with HU-SDS–PAGE sample buffer (8 M urea, 200 mM NaH_2PO_4, pH 6.8, 5% SDS, 0.1 mM EDTA, 0.1% bromophenol blue) at 42°C for 15 min. The supernatant was mixed with 1,4-dithiothreitol (DTT) (final concentration 25 mM) and subjected to SDS–PAGE followed by immunoblotting.

A basic cell fractionation assay was performed for the carbonate extraction assay. Cells in the exponential growth phase (culture size 50 ml) were harvested, washed with 4 ml of cold water containing 1 mM PMSF and 10 mM NaN_3, and lysed with glass beads in lysis buffer (0.7 M sorbitol, 50 mM Tris/HCl, pH 7.5). Cell debris was removed by centrifugation (500 × *g*, 5 min) and the supernatant was treated with lysis buffer, Na_2CO_3 (0.1 M final concentration), or Triton X-100 (1% final concentration) for 30 min on ice. Pellet and supernatant fraction were separated by centrifugation (20,000 × g, 45 min, 4°C) and proteins of the supernatant were precipitated with TCA (final concentration 10%). The precipitates of the pellet and the supernatant fractions were dissolved in HU-SDS–PAGE sample buffer containing DTT and subjected to SDS–PAGE followed by immunoblotting.

Quantification data obtained with Fiji were imported into the software LibreOffice Calc. The mean and the SEM were calculated from at least three independent experiments (biological replicates). If applicable, statistical significance was calculated using a two-sided Student's *t* test with LibreOffice Calc.

Fluorescence microscopy and flow cytometer measurements

Fluorescence microscopy of living yeast cells was performed as described (Jungbluth *et al.*, 2010) with a Zeiss Axiovert 200 equipped with a Hamamatsu camera, EGFP and rhodamine filter sets, and a 63x Plan Apochromat oil lens (NA 1.4). Transmission light and fluorescence images were collected in a single plane using the image acquisition software Volocity 5.03 (Perkin Elmer, Waltham, MA). The software Fiji was used for image processing and fluorescence quantification (Schindelin *et al.*, 2012). Flow cytometer measurements were performed as described by Hasenjäger *et al.* (2019). Briefly, yeast cells in logarithmic growth phase were treated with sodium azide (10 mM final concentration) and transferred to a 96-well plate. The measurements were performed with an Attune NxT (ThermoFisher) equipped with an autosampler. Mean red fluorescence of six independent measurements was used to generate the graph; error bars shows the SEM.

ACKNOWLEDGMENTS

We thank Daniela Störmer for her excellent technical assistance and J. Dohmen, M.H. Glickman, M. Hochstrasser, T. Sommer, and D. Wolf for yeast strains. This work was supported by Deutsche Forschungsgemeinschaft (DFG) Grant TA320/7-1 and Bundesministerium für Bildung und Forschung (BMBF) Grant 031B0358A.

REFERENCES

Bagola K, Mehnert M, Jarosch E, Sommer T (2011). Protein dislocation from the ER. Biochim Biophys Acta 1808, 925–936.

Bar-Nun S, Glickman MH (2012). Proteasomal AAA-ATPases: structure and function. Biochim Biophys Acta 1823, 67–82.

Bays NW, Wilhovsky SK, Goradia A, Hodgkiss-Harlow K, Hampton RY (2001). HRD4/NPL4 is required for the proteasomal processing of ubiquitinated ER proteins. Mol Biol Cell 12, 4114–4128.

Brachmann CB, Davies A, Cost GJ, Caputo E, Li J, Hieter P, Boeke JD (1998). Designer deletion strains derived from *Saccharomyces cerevisiae* S288C: a useful set of strains and plasmids for PCR-mediated gene disruption and other applications. Yeast 14, 115–132.

Braun S, Matuschewski K (2002). Role of the ubiquitin-selective CDC48UFD1/NPL4 chaperone (segregase) in ERAD of OLE1 and other substrates. EMBO J 21, 615–621.

Braunger K, Pfeffer S, Shrimal S, Gilmore R, Berninghausen O, Mandon EC, Becker T, Förster F, Beckmann R (2018). Structural basis for coupling protein transport and N-glycosylation at the mammalian endoplasmic reticulum. Science 360, 215–219.

Ciechanover A (2005). Proteolysis: from the lysosome to ubiquitin and the proteasome. Nat Rev Mol Cell Biol 6, 79–87.

Cuanalo-Contreras K, Mukherjee A, Soto C (2013). Role of protein misfolding and proteostasis deficiency in protein misfolding diseases and aging. Int J Cell Biol 2013, 638083.

Erales J, Coffino P (2014). Ubiquitin-independent proteasomal degradation. Biochim Biophys Acta 1843, 216–221.
Erales J, Hoyt MA, Troll F, Coffino P (2012). Functional asymmetries of proteasome translocase pore. J Biol Chem 287, 18535–18543.
Ferreira T, Brett Mason A, Pypaert M, Allen KE, Slayman CW, Mason AB, Pypaert M, Allen KE, Slayman CW (2002). Quality control in the yeast secretory pathway: a misfolded PMA1 H+-ATPase reveals two checkpoints. J Biol Chem 277, 21027–21040.
Finke K, Plath K, Panzner S, Prehn S, Rapoport TA, Hartmann E, Sommer T (1996). A second trimeric complex containing homologs of the Sec61p complex functions in protein transport across the ER membrane of *S. cerevisiae*. EMBO J 15, 1482–1494.
Gietz D, St Jean A, Woods RA, Schiestl RH (1992). Improved method for high efficiency transformation of intact yeast cells. Nucleic Acids Res 20, 1425.
Gödderz D, Schäfer E, Palanimurugan R, Dohmen RJ (2011). The N-terminal unstructured domain of yeast ODC functions as a transplantable and replaceable ubiquitin-independent degron. J Mol Biol 407, 354–367.
Gross LA, Baird GS, Hoffman RC, Baldridge KK, Tsien RY (2000). The structure of the chromophore within DsRed, a red fluorescent protein from coral. Proc Natl Acad Sci USA 97, 11990–11995.
Han S, Liu Y, Chang A (2007). Cytoplasmic Hsp70 promotes ubiquitination for endoplasmic reticulum-associated degradation of a misfolded mutant of the yeast plasma membrane ATPase, PMA1. J Biol Chem 282, 26140–26149.
Hasenjäger S, Trauth J, Hepp S, Goenrich J, Essen, L-O, Taxis C (2019). Optogenetic downregulation of protein levels with an ultrasensitive switch. ACS Synth Biol 8, 1026–1036.
Hermann A, Liewald JF, Gottschalk A (2015). A photosensitive degron enables acute light-induced protein degradation in the nervous system. Curr Biol 25, R749–R750.
Itskanov S, Park E (2018). Structure of the posttranslational Sec protein-translocation channel complex from yeast. Science 363, 1–9.
Janke C, Magiera MM, Rathfelder N, Taxis C, Reber S, Maekawa H, Moreno-Borchart A, Doenges E, Schwob E, Schiebel E, *et al.* (2004). A versatile toolbox for PCR-based tagging of yeast genes: new fluorescent proteins, more markers and promoter substitution cassettes. Yeast 21, 947–962.
Jarosch E, Taxis C, Volkwein C, Bordallo J, Finley D, Wolf DH, Sommer T (2002). Protein dislocation from the ER requires polyubiquitination and the AAA-ATPase Cdc48. Nat Cell Biol 4, 134–139.
Jungbluth M, Renicke C, Taxis C (2010). Targeted protein depletion in *Saccharomyces cerevisiae* by activation of a bidirectional degron. BMC Syst Biol 4, 176.
Lee RJ, Liu CW, Harty C, McCracken AA, Latterich M, Römisch K, DeMartino GN, Thomas PJ, Brodsky JL (2004). Uncoupling retro-translocation and degradation in the ER-associated degradation of a soluble protein. EMBO J 23, 2206–2215.
Lipson C, Alalouf G, Bajorek M, Rabinovich E, Atir-Lande A, Glickman M, Bar-Nun S (2008). A proteasomal ATPase contributes to dislocation of endoplasmic reticulum-associated degradation (ERAD) substrates. J Biol Chem 283, 7166–7175.
Lutz AP, Renicke C, Taxis C (2016). Controlling protein activity and degradation using blue light. In: Methods in Molecular Biology, ed. A Kianianmomeni, New York: Humana Press, 67–78.
Mayer TU, Braun T, Jentsch S (1998). Role of the proteasome in membrane extraction of a short-lived ER-transmembrane protein. EMBO J 17, 3251–3257.
Metzger MB, Maurer MJ, Dancy BM, Michaelis S (2008). Degradation of a cytosolic protein requires endoplasmic reticulum-associated degradation machinery. J Biol Chem 283, 32302–32316.
Morris LL, Hartman IZ, Jun DJ, Seemann J, DeBose-Boyd RA (2014). Sequential actions of the AAA-ATPase valosin-containing protein (VCP)/p97 and the proteasome 19 S regulatory particle in sterol-accelerated, endoplasmic reticulum (ER)-associated degradation of 3-hydroxy-3-methylglutarylcoenzyme a reductase. J Biol Chem 289, 19053–19066.
Nakatsukasa K, Brodsky JL, Kamura T (2013). A stalled retrotranslocation complex reveals physical linkage between substrate recognition and proteasomal degradation during ER-associated degradation. Mol Biol Cell 24, 1765–1775.
Nakatsukasa K, Huyer G, Michaelis S, Brodsky JL (2008). Dissecting the ER-associated degradation of a misfolded polytopic membrane protein. Cell 132, 101–112.
Palanimurugan R, Scheel H, Hofmann K, Jürgen Dohmen R (2004). Polyamines regulate their synthesis by inducing expression and blocking degradation of ODC antizyme. EMBO J 23, 4857–4867.
Pereira G, Tanaka TU, Nasmyth K, Schiebel E (2001). Modes of spindle pole body inheritance and segregation of the Bfa1p-Bub2p checkpoint protein complex. EMBO J 20, 6359–6370.
Preston GM, Brodsky JL (2017). The evolving role of ubiquitin modification in endoplasmic reticulum-associated degradation. Biochem J 474, 445–469.
Rabinovich E, Kerem A, Fröhlich, K-U, Diamant N, Bar-Nun S (2002). AAA-ATPase p97/Cdc48p, a cytosolic chaperone required for endoplasmic reticulum-associated protein degradation. Mol Cell Biol 22, 626–634.
Rape M, Jentsch S (2004). Productive RUPture: activation of transcription factors by proteasomal processing. Biochim Biophys Acta 1695, 209–213.
Ravid T, Hochstrasser M (2008). Diversity of degradation signals in the ubiquitin–proteasome system. Nat Rev Mol Cell Biol 9, 679–689.
Ravid T, Kreft SG, Hochstrasser M (2006). Membrane and soluble substrates of the Doa10 ubiquitin ligase are degraded by distinct pathways. EMBO J 25, 533–543.
Rendueles P, Wolf D (1988). Proteinase function in yeast: biochemical and genetic approaches to a central mechanism of post-translational control in the eukaryote cell. FEMS Microbiol Lett 54, 17–45.
Renicke C, Schuster D, Usherenko S, Essen LO, Taxis C (2013). A LOV2 domain-based optogenetic tool to control protein degradation and cellular function. Chem Biol 20, 619–626.
Römisch K (2017). A case for Sec61 channel involvement in ERAD. Trends Biochem Sci 42, 171–179.
Rubenstein EM, Kreft SG, Greenblatt W, Swanson R, Hochstrasser M (2012). Aberrant substrate engagement of the ER translocon triggers degradation by the Hrd1 ubiquitin ligase. J Cell Biol 197, 761–773.
Rubin DM, Glickman MH, Larsen CN, Dhruvakumar S, Finley D (1998). Active site mutants in the six regulatory particle ATPases reveal multiple roles for ATP in the proteasome. EMBO J 17, 4909–4919.
Schindelin J, Arganda-Carreras I, Frise E, Kaynig V, Longair M, Pietzsch T, Preibisch S, Rueden C, Saalfeld S, Schmid B, *et al.* (2012). Fiji: an open-source platform for biological-image analysis. Nat Methods 9, 676–682.
Sherman F (2002). Getting started with yeast. Methods Enzymol 350, 3–41.
Stolz A, Wolf DH (2010). Endoplasmic reticulum associated protein degradation: a chaperone assisted journey to hell. Biochim Biophys Acta 1803, 694–705.
Swanson R, Locher M, Hochstrasser M (2001). A conserved ubiquitin ligase of the nuclear envelope/endoplasmic reticulum that functions in both ER-associated and Mat α 2 repressor degradation. Genes Dev 2, 2660–2674.
Taxis C, Hitt R, Park S-H, Deak PM, Kostova Z, Wolf DH (2003). Use of modular substrates demonstrates mechanistic diversity and reveals differences in chaperone requirement of ERAD. J Biol Chem 278, 35903-35913.
Trauth J, Scheffer J, Hasenjäger S, Taxis C (2019). Synthetic control of protein degradation during cell proliferation and developmental processes. ACS Omega 4, 2766–2778.
Usherenko S, Stibbe H, Muscò, M, Essen LO, Kostina EA, Taxis C (2014). Photo-sensitive degron variants for tuning protein stability by light. BMC Syst Biol 8, 128.
Vilchez D, Saez I, Dillin A (2014). The role of protein clearance mechanisms in organismal ageing and age-related diseases. Nat Commun 5, 1–13.
Voorhees RM, Fernández IS, Scheres SHW, Hegde RS (2014). Structure of the mammalian ribosome–Sec61 complex to 3.4 Å resolution. Cell 157, 1632–1643.
Walter J, Urban J, Volkwein C, Sommer T (2001). Sec61p-independent degradation of the tail-anchored ER membrane protein Ubc6p. EMBO J 20, 3124–3131.
Weber A, Cohen I, Popp O, Dittmar G, Reiss Y, Sommer T, Ravid T, Jarosch E (2016). Sequential poly-ubiquitylation by specialized conjugating enzymes expands the versatility of a quality control ubiquitin ligase. Mol Cell 63, 827–839.
Wilkinson BM, Critchley AJ, Stirling CJ (1996). Determination of the transmembrane topology of yeast Sec61p, an essential component of the endoplasmic reticulum translocation complex. J Biol Chem 271, 25590–25597.

Wu X, Cabanos C, Rapoport TA (2019). Structure of the post-translational protein translocation machinery of the ER membrane. Nature 566, 136–139.
Ye Y, Meyer HH, Rapoport TA (2001). The AAA ATPase Cdc48/p97 and its partners transport proteins from the ER into the cytosol. Nature 414, 652–656.
Ye Y, Tang WK, Zhang T, Xia D (2017). A mighty "protein extractor" of the cell: structure and function of the p97/CDC48 ATPase. Front Mol Biosci 4, 1–20.
Zattas D, Berk JM, Kreft SG, Hochstrasser M (2016). A conserved c-terminal element in the yeast doa10 and human march6 ubiquitin ligases required for selective substrate degradation. J Biol Chem 291, 12105–12118.
Zattas D, Hochstrasser M (2015). Ubiquitin-dependent protein degradation at the yeast endoplasmic reticulum and nuclear envelope. Crit Rev Biochem Mol Biol 50, 1–17.
Zhang Y, Nijbroek G, Sullivan ML, McCracken AA, Watkins SC, Michaelis S, Brodsky JL (2001). Hsp70 molecular chaperone facilitates endoplasmic reticulum-associated protein degradation of cystic fibrosis transmembrane conductance regulator in yeast. Mol Biol Cell 12, 1303–1314.